JOC The Journal of Organic Chemistry

Article

pubs.acs.org/joc

Mechanistic Investigation of Enediyne-Connected Amino Ester Rearrangement. Theoretical Rationale for the Exclusive Preference for 1,6- or 1,5-Hydrogen Atom Transfer Depending on the Substrate. A Potential Route to Chiral Naphthoazepines

Damien Campolo,[†] Anouk Gaudel-Siri,*[,†] Shovan Mondal,[†] Didier Siri,[†] Eric Besson,[†] Nicolas Vanthuyne,[‡] Malek Nechab,*[,†] and Michèle P. Bertrand*[,†]

[†]Institut de Chimie Radicalaire, CNRS UMR 7273, Equipes CMO and CTM, and [‡]ISM2, CNRS UMR 7313, Equipe Chirosciences, Aix-Marseille Université, 13397 Cedex 20, Marseille, France

Supporting Information

ABSTRACT: Memory of chirality (MOC) and deuterium-labeling studies were used to demonstrate that the cascade rearrangement of enediyne-connected amino esters **1a** and **1b** evolved through exclusive 1,5- or 1,6-hydrogen atom transfer, subsequent to 1,3-proton shift and Saito−Myers cyclization, depending on the structure of the starting material. These results were independently confirmed by DFT theoretical calculations performed on model monoradicals. These calculations clearly demonstrate that in the alanine series, 1,5-hydrogen shift is kinetically favored over 1,6-hydrogen shift because of its greater exergonicity. In the valine series, the bulk of the substituent at the nitrogen atom has a major influence on the fate of the reaction. *N*-Tosylation increases the barrier to 1,5-hydrogen shift to the benefit of 1,6-hydrogen shift. The ready availability of 1,6-hydrogen atom transfer was explored as a potential route for the enantioselective synthesis of naphthoazepines.

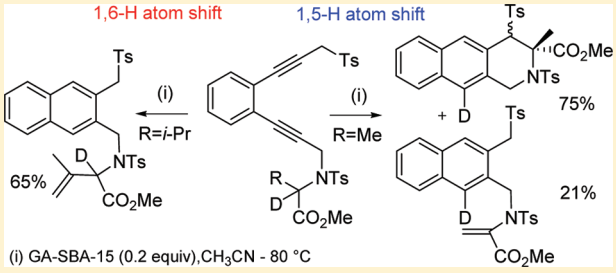

INTRODUCTION

We have recently reported the enantioselective cascade rearrangement of enediyne **1a** which evolved through the mechanism depicted in Scheme 1.[1,2] The reaction proceeded with memory of chirality[3] and retention of the configuration of the starting material owing to the generation of intermediate **C** in a chiral conformation. The racemization half-life time of the captodative center in diradical **C** is long compared to the time scale of the recombination step (d). By opposition to enantiopure enediynes in which the stereogenic center was included in a 5-membered ring,[1,2] substrate **1a** led to an undesired olefinic product (**3a**) that resulted from a disproportionation step (e),[4] which competed with the biradical recombination leading to tetrahydrobenzoisoquinolines **2a**. These reactions that were initially performed using alumina as the base were shown to proceed very readily with a recoverable nanocatalyst, i.e., mesoporous silica grafted with a tertiary amino group (GA-SBA-15).[5] Overall yields were significantly improved, and the reaction could be carried out indifferently in benzene or in acetonitrile. The main drawback in this methodology was the lack of diastereoselectivity which resulted in the formation of two enantioenriched diastereomers with two contiguous stereocenters. This drawback was very recently overcome by designing a one-pot strategy.[6] Tandem Crabbé homologation (leading to monosubstituted allenes)/Myers−Saito cyclization-induced rearrangement was shown to lead to heterocyclic compounds bearing only one stereocenter that was nearly totally controlled by the MOC phenomenon. We discuss herein the comparative behavior of structurally related enediynes derived from valine and alanine, respectively.

RESULTS AND DISCUSSION

Synthetic Results. When enediyne (*S*)-**1b** was submitted to similar experimental conditions (in the presence of 0.2 equiv of GA-SBA-15), (*S*)-**4b** was isolated as the only product at the expense of any tricyclic product issued from a recombination process (eq 1). Intrigued by the formation of olefin **4b**, while **3b** was expected on the ground of the common prevalence of 1,5-hydrogen shifts, we have checked the influence of other experimental conditions on the fate of (*rac*)-**1b**. In the presence of an excess of base, **3b** could also be formed, but indirectly. It resulted from **4b** through the slow migration of the double bond (eq 2).

It became obvious that **4b** was the kinetic product and, therefore, that it resulted from 1,6-hydrogen atom transfer rather than from 1,5-transfer of the hydrogen atom in captodative position.

The kinetic preference for 1,6-hydrogen shift was unambiguously demonstrated by measuring the optical purity of **4b** generated as the unique reaction product from optically pure **1b** (ee >99%) (eq 1); the reaction proceeded without loss of

Received: December 21, 2011
Published: February 16, 2012

   dx.doi.org/10.1021/jo202580y | *J. Org. Chem.* 2012, 77, 2773−2783

Scheme 1. General Mechanism

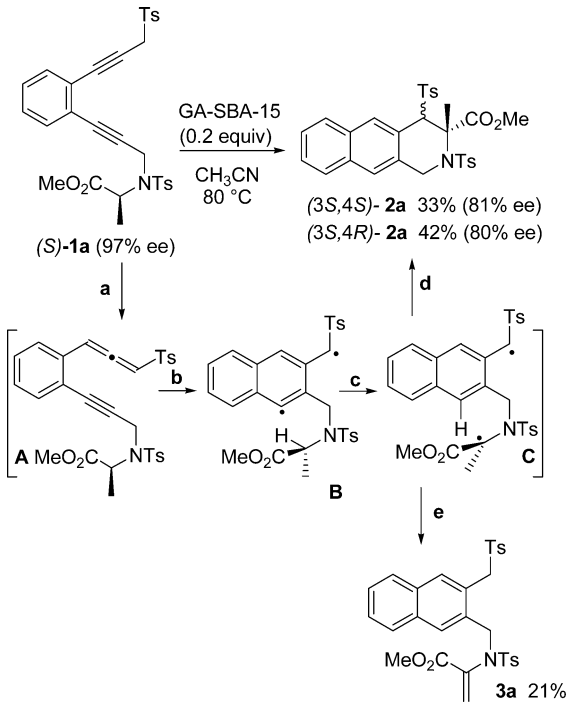

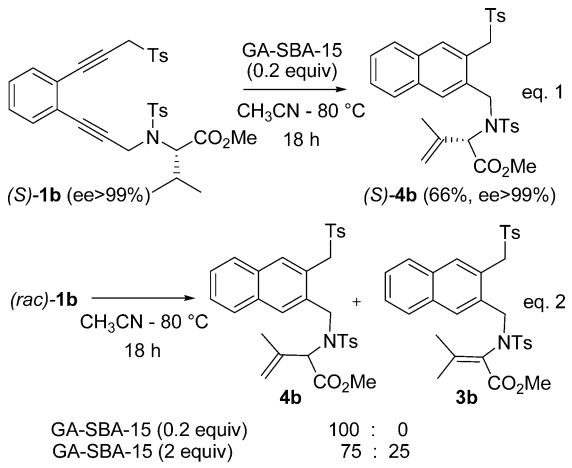

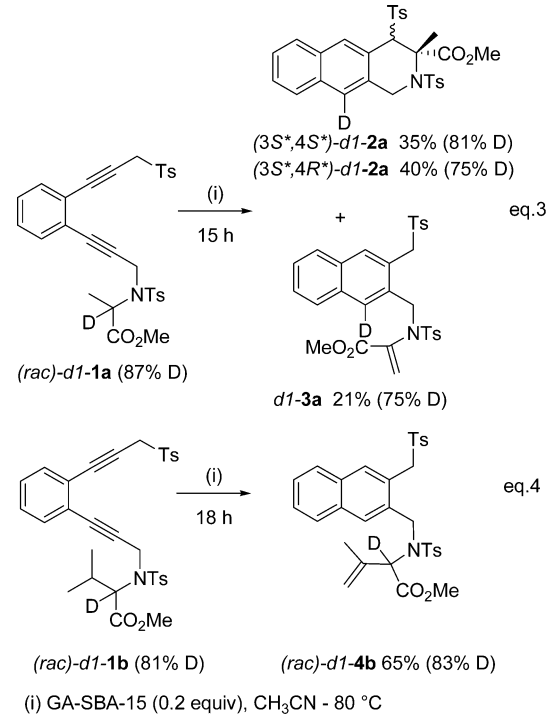

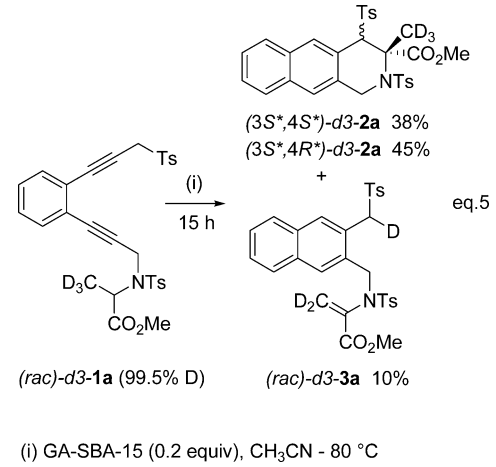

chirality. The enantiopurity of the starting material was entirely recovered in the product.

The formation of **3a** through 1,5-hydrogen shift to 1-naphthyl radical **B** (Scheme 1) was therefore questioned. The pathways leading to **3a** and **3b** were confirmed by deuterium labeling of substrates **1a** and **1b** as reported in eqs 3−5, respectively.

Racemic **1a** and **1b**, monodeuterated at the captodative position, were prepared from monodeuterated racemic *N*-tosylalanine and *N*-tosylvaline methyl esters, respectively. Deuteration of the precursors was accomplished upon treatment with K_2CO_3 in MeOD (99% D) at 70 °C (see the Supporting Information).

As shown in eq 3, both monodeuterated products **2a** and **3a** resulting from the rearrangement of (*rac*)-*d1*-**1a** were labeled exclusively at the aromatic ring, as expected from exclusive 1,5-hydrogen shift. The rate of deuteration with respect to the starting material was determined from the relative area of the residual singlet signal of the unlabeled aromatic proton. Errors originating from the integration of aromatic signals are probably responsible for the gap between the effective and the theoretical rate of deuteration.[7] Conversely, as shown in eq 4, the unique product resulting from (*rac*)-*d1*-**1b**, i.e., (*rac*)-*d1*-**4b**, was exclusively deuterated at the captodative position, which confirmed that in this case only 1,6-hydrogen shift had occurred.

The rearrangement of (*rac*)-*d3*-**1a**, prepared from the corresponding commercially available (*rac*)-*d3*-alanine (99.5% D), is reported in eq 5. It corroborated the results reported in eq 3. Deuterium was recovered exclusively in the CD_3 group in the tricyclic diastereomeric products ((*rac*)-*d3*-**2a**). In addition, in *d3*-**3a** deuterium was scrambled between the terminal olefinic carbon and the methylene group of the benzylic sulfone. In all likelihood, disproportionation is an intramolecular pathway.

An interesting feature was noted. The relative ratio of isolated products (3*S*,4*S*)-**2a**:(3*S*,4*R*)-**2a**:**3a** that was initially 42:33:21 (Scheme 1) or 40:35:21 (eq 3)[5] became 45:38:10 in the experiment performed on (*rac*)-*d3*-**1a** (eq 5). A primary kinetic isotope effect slowed down disproportionation and

dx.doi.org/10.1021/jo202580y | J. Org. Chem. 2012, 77, 2773−2783

Chart 1

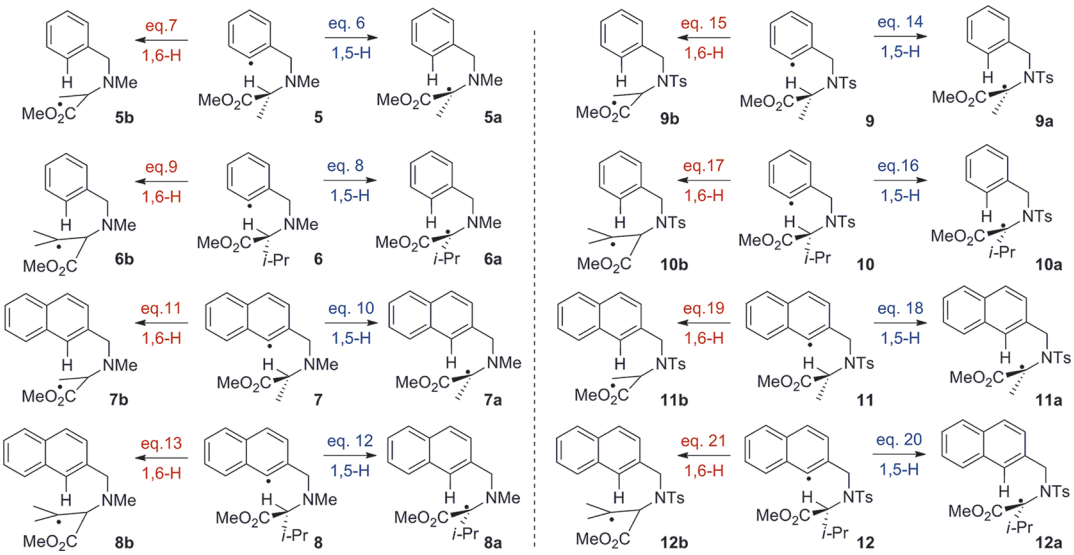

increased the global yield of tricyclic products from 75 to 83% at the expense of *d3*-**3a**.[8] It is to be noted that apparently disproportionation affected similarly the pathways leading to both diastereomers (the ratio of which remained constant within the limits of experimental errors).

Examples of 1,5-hydrogen abstraction are widespread in the literature. Applications of Barton and Hoffmann−Loeffler reactions, based on *O*- and *N*-centered radicals, respectively, are well documented.[9] Similarly, many synthetic strategies are based on radical translocation from vinyl or aryl radicals which have become very popular and powerful synthetic tools.[9c,d,10] Comparatively, examples of 1,6-hydrogen shift are less numerous.[11]

Peculiar attention was given to literature data where 1,5- and 1,6-hydrogen shifts could be competitive pathways.[12−14] As a rule of thumb, 1,5-hydrogen shift is generally favored over 1,6-hydrogen shift. According to theoretical calculations based on butoxy and pentoxy radical, the preference for 1,5-hydrogen shift (six-membered ring transition state) over 1−6 hydrogen shift (seven-membered ring transition sate), results from the more favorable activation entropy of the former. Activation enthalpy of the rearrangement of pentoxy radical was found only 0.7 kcal per mole lower than that of butoxy radical.[15] Exceptions to the rule occur when 1,6-hydrogen shift is more exothermic than 1,5-migration, however, in most cases, mixtures of products resulting from the competition between these two processes were formed.

The unique example of recent theoretical calculations using B3LYP DFT functional, and concerning independent 1,5- and 1,6-hydrogen abstractions by aryl radical, deals with the methodology developed by Curran[13] from *o*-iodoanilide derivatives.[16,17]

According to Schiesser data, the rate constant for 1,5-hydrogen transfer from a captodative position in such structures ranges between 1.0 and 4.9 × 10^7 s^{-1}.[18] In the very same paper, the authors have observed that 1,6- or 1,7-radical translocations competed with 1,5- hydrogen shift depending on the structure. However, these structures are completely different from ours, particularly in regard of the planarity of the anilide moiety and extrapolations to the fate of radicals of type **B** (Scheme 1) might be hazardous.

The only data found in the literature concerning 1-naphthyl radicals have been reported by De Mesmaeker.[14,19] The latter also mentioned competitive 1,5-, 1,6-, and 1,7-H transfers, but even these results cannot be correlated to ours, since in these reactions, 1-naphthyl radicals abstracted hydrogen atoms from an aliphatic chain located in position 8 and not in position 2.

The above disclosed rearrangement of **1b** was rather surprising since 1,6-hydrogen shift is kinetically favored to the exclusion of any 1,5-hydrogen shift, even though the latter should be more, or at least, as exothermic as the previous one. DFT calculations were undertaken on model monoradicals to confirm or infirm these observations.

Computational Section. First the translocation reaction was investigated starting from simple models, i.e., radicals **5**−**8** bearing a methyl group as substituent at nitrogen, for the sake of reducing calculation time (Chart 1, eqs 6−13). Then, based on these data, new explorations of the potential energy surface were achieved to calculate the transition state geometries for the rearrangements of *N*-tosylated monoradicals **9**−**12** (Chart 1, eqs 14−21). The latter are closely related to the intermediate biradicals involved in the enediynes cascade transformation.

Computational Details. DFT calculations were performed to determine the profiles of the competitive reactions using the Gaussian 09 program.[20] The geometries were fully optimized at the UB3LYP/6-31G(d) level of theory. Vibrational frequencies were calculated at the UB3LYP/6-31G(d) level to determine the nature of the located stationary points. Zero-point energies and thermodynamic data were calculated using the specified scaling factor (0.9603).[21] All transition-state geometries were confirmed by intrinsic reaction coordinates (IRC) calculations. In order to enhance the accuracy of the calculations, single-point energies were calculated at the UB3LYP/6-311++G-(3df,3pd) level of theory. The spin contamination was low for all radical species (<S^2> values ranged between 0.754 and 0.760).

Some model reactions (Chart 1, eqs 6−9) were also calculated at the G3(MP2)-RAD level of theory to validate the selection of UB3LYP/6-311++G(3df,3pd)//UB3LYP/6-31G(d) method. B3LYP methods are known to underestimate energies values, however the energy gaps are consistent with those obtained from G3(MP2)-RAD calculations which are

dx.doi.org/10.1021/jo202580y | *J. Org. Chem.* 2012, 77, 2773−2783

known to be highly reliable for radical species (Figure 1, Table 1).[22]

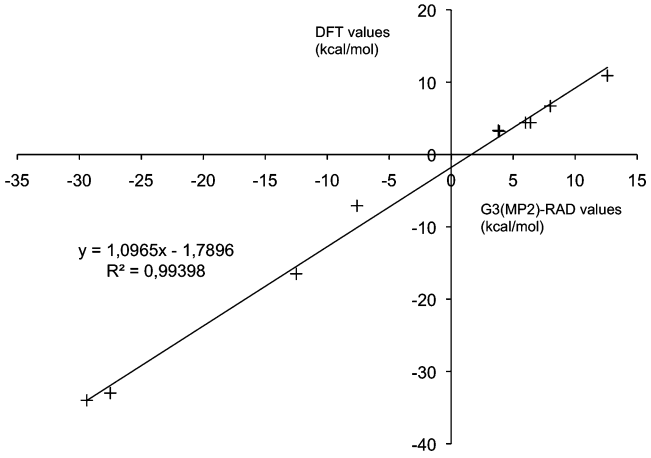

Figure 1. Linear correlation between free energy values calculated at the UB3LYP/6-311++G(3df,3pd)//UB3LYP/6-31G(d) and the G3-(MP2)-RAD levels.

Computational Data. The activation free energy ($\Delta G^{\ddagger}$), the activation enthalpy ($\Delta H^{\ddagger}$), and entropy ($\Delta S^{\ddagger}$), together with the reaction exergonicity (ΔG_0) are reported in Table 1 for each reaction (Chart 1, eqs 6−21). It must be noticed that the intrinsic reaction coordinate (IRC) calculations led, in most cases, to slightly different conformations of the reactive starting radical depending on the nature of the transition state (six- or seven-membered ring). The free energy differences ΔG_{conf} between these conformers of the starting radical are given in Table 1. The conformations obtained from the seven-membered transition states are the least stable ones for *N*-methylated model radicals and the situation is reversed for *N*-tosylated radicals. IRC calculations show that the conformer predisposed to 1,5-H shift is less stable than the conformer predisposed to 1,6-H shift, in the case of radicals **9**, **10** and **12**. No energy difference is observed in the case of radical **11** (see ΔG_{conf} in Table 1).

The predicted ratio of products **Xa** and **Xb** (X = 5−12), issued from the competitive 1,5- and 1,6-H shift reactions, respectively, are given in Table 1 (they were determined from the calculated $\Delta\Delta G^{\ddagger}$ values). From the calculations performed on the series of *N*-methyl model radicals derived from alanine (radicals **5** and **7**), 1,5-H transfer is obviously much faster than 1,6-H transfer (see $\Delta G^{\ddagger}$ in Table 1). It must be noted that the least stable conformer (ready to undergo 1,6-H shift from the methyl group) of any of these starting radicals should account for less than 1% at 298 K according to Boltzmann partition.

According to theoretical calculations, 1,5-H transfer remains favored over 1,6-H transfer, even in the valine series (radicals **6**, **8**), but the barrier for 1,6-hydrogen shift is decreased as compared to the alanine series (the incidence of the reaction exergonicity is discussed in the following). Both aryl and 1-naphthyl radicals behave similarly.

In this first series of model radicals, i.e., *N*-methyl derivatives, in all cases, 1,6-H shift is enthalpically disfavored and the activation enthalpic governs the fate of the radical, although the activation entropy is more favorable for the seven-membered ring transition state ($\Delta S^{\ddagger}$ values show that the six-membered ring transition state geometry for 1,5-H transfer is more constrained in most cases but radical **8**).

It must be noted that, not surprisingly, the homolysis of the captodative C−H bond corresponds to the most exergonic reactions (see $\Delta\Delta G_0$ in Table 1). Due to the difference between the bond dissociation energy (BDE) of the C−H bond in the methyl group and that of the tertiary C−H bond in the isopropyl group the enthalpic factors should contribute to a lesser extend to the activation barrier in the case of valine derivatives.

The captodative character of radicals **9**−**12** may be questioned,[23] and the simple comparison of the calculated free energy of reactions (ΔG_0) involving 1,5-H migration, i.e.,

Table 1. ΔG_{conf}, $\Delta G^{\ddagger}$, $\Delta\Delta G^{\ddagger}$, $\Delta H^{\ddagger}$, ΔG_0, $\Delta\Delta G_0$, and $\Delta G^{\ddagger}_i$ in kcal/mol and $\Delta S^{\ddagger}$ in cal/mol/K, for 1,5- and 1,6- Translocations of Radicals 5−12, Calculated at 298 K at the UB3LYP/6-311++G(3df,3pd)//UB3LYP/6-31G(d) Level of Theory

reaction	ΔG_{conf} [b]	$\Delta G^{\ddagger}$ [a−c]	$\Delta\Delta G^{\ddagger}$ [d] (X_a/X_b)	$\Delta H^{\ddagger}$	$\Delta S^{\ddagger}$	ΔG_0 [a−c]	$\Delta\Delta G_0$ [e]	$\Delta G^{\ddagger}_i$
5→5a	0.0	4.4 (6.4)	−6.5 (5.8×10^4)	2.8	−5.5	−34.0 (−29.4)	−26.9	17.2
5→5b	3.2 (3.9)	10.9 (12.6)		10.0	−2.9	−7.1 (−7.6)		12.3
6→6a	0.0	4.4 (6.0)	−2.3 (49)	2.3	−6.9	−33.0 (−27.5)	−16.5	16.8
6→6b	3.3 (3.8)	6.7 (8.0)		5.0	−5.6	−16.5 (−12.5)		11.1
7→7a	0.0	3.6	−7.3 (2.2×10^5)	1.9	−5.8	−34.4	−26.8	16.2
7→7b	2.7	10.9		9.6	−4.5	−7.6		12.8
8→8a	0.0	4.2	−3.3 (2.6×10^2)	1.4	−9.4	−31.6	−14.7	16.2
8→8b	2.0	7.5		4.6	−9.7	−16.9		12.6
9→9a	0.9	5.3	−2.6 (81)	3.7	−5.3	−28.1	−17.8	15.5
9→9b	0.0	7.9		6.2	−5.7	−10.3		12.5
10→10a	3.5	9.0	4.2 (8.3×10^{-4})	8.2	−2.6	−22.2	−0.5	15.7
10→10b	0.0	4.8		5.5	+2.4	−21.7		13.5
11→11a	0.0	3.8	−4.3 (1.4×10^3)	2.7	−3.6	−26.9	−15.8	14.1
11→11b	0.0	8.1		6.2	−6.4	−11.1		13.1
12→12a	5.2	10.8	3.3 (3.8×10^{-3})	8.4	−7.9	−20.9	−0.2	16.0
12→12b	0.0	7.5		6.1	−4.6	−20.7		16.2

[a]G3(MP2)-RAD values are given in parentheses. [b]Free energy difference between the two most stable conformers of radicals **5**−**12** resulting from IRC calculations. [c]Free energies of the competitive 1,5- and 1,6-hydrogen atom transfers are given relative to the most stable conformer. [d]$\Delta\Delta G^{\ddagger} = \Delta G^{\ddagger}_{(1,5\text{-H})} - \Delta G^{\ddagger}_{(1,6\text{-H})}$, **Xa**/**Xb** = $e^{-\Delta\Delta G^{\ddagger}/RT}$ is the product ratio resulting from the competitive 1,5- and 1,6-hydrogen atom transfers. [e]$\Delta\Delta G_0 = \Delta G_{0(1,5\text{-H})} - \Delta G_{0(1,6\text{-H})}$.

dx.doi.org/10.1021/jo202580y | J. Org. Chem. 2012, 77, 2773−2783

5→5a/9→9a, 6→6a/10→10a, 7→7a/11→11a, 8→8a/12→12a, shows that the stabilization energy of radicals bearing a *N*-Ts group at nitrogen is lower than that of radicals bearing a *N*-Me group by 5.9 to 10.9 kcal/mol. However, it is difficult to estimate the relative contribution of electronic and steric effects.[24]

In agreement with Hammond's postulate,[25] the activation free energy is influenced by the reaction exergonicity. In Marcus formalism,[26] the activation free energy ($\Delta G^{\ddagger}$) is the sum of an intrinsic activation free energy ($\Delta G^{\ddagger}_{i}$) and a thermodynamic contribution including the reaction free enthalpy (ΔG_0) (Figure 2). The intrinsic barrier represents

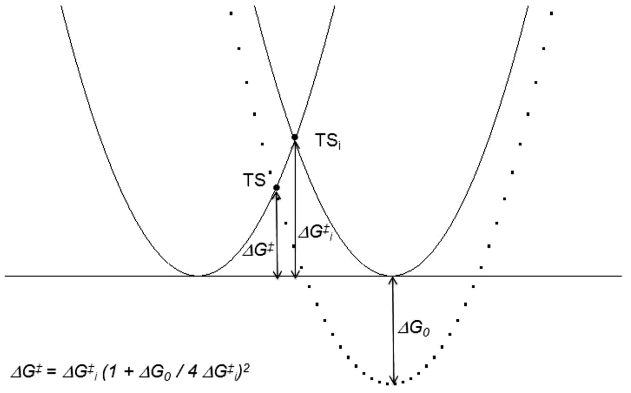

Figure 2. Relationships between ΔG_0, $\Delta G^{\ddagger}$, and $\Delta G^{\ddagger}_i$ in Marcus formalism.

pure transition states effects for thermoneutral process. The thermodynamic contribution lowers the activation free energy for exergonic processes, or conversely increases the activation free energy for endergonic reactions.

The values of the intrinsic barriers ($\Delta G^{\ddagger}_i$) clearly indicate that 1,6-hydrogen shift should be largely favored over 1,5-hydrogen shift in nearly all cases but radicals **11** and **12**, for which a competition should be expected between the two reactions. The exergonicity driving force is responsible for the lowering of the activation free energy and for the exclusive preference for 1,5-H shift predicted in the case of radicals **5**−**9**.

Due to the higher exergonicity of the process, the transition state of 1,5-H migration is earlier than that of 1,6-H shift, which should alleviate steric crowding. The C−H distances in the corresponding transition structures are given in Table 2, where *L* (eq 22) is a measure of the precocity of the transition state.[27] As expected in the alanine series, the transition state for 1,5-H shift is much earlier than the transition state for 1,6-H shift; the difference in *L* parameters is less pronounced in the valine series.

$$L = \frac{d(C\cdots H)^{\ddagger} - d(C\cdots H)_{rad}}{d(C_{Ar}\cdots H)^{\ddagger} - d(C_{Ar}\cdots H)_{product}} \qquad (22)$$

Calculations suggest that the nature of the substituent at nitrogen has a determining influence on the kinetics of the two competitive reactions. In the case of *N*-tosyl derivatives the situation becomes strongly dependent on the nature of the amino ester moiety. In the alanine series (radicals **9** and **11**), whatever the structure of the radical (aryl or 1-naphthyl), and even though 1,6-H shift remains intrinsically favored ($\Delta G^{\ddagger}_i$ in Table 1), 1,5-H shift is much faster owing to the high exergonicity of this process ($\Delta G^{\ddagger}$ and ΔG_0 in Table 1).

Table 2. Calculated C−H Distances (in Å) in the Transition States for 1,5- And 1,6-translocations of radicals 5−12 at the UB3LYP/6-311++G(3df,3pd)//(UB3LYP/6-31G(d) Level at 298 K

reaction	*d*(C···H)	*d*(C−H) (substrate)	*d*(C_{Ar}···H)	*d*(C_{Ar}−H) product	*L*
5→5a	1.234	1.097	1.505	1.086	0.327
5→5b	1.286	1.104	1.399	1.087	0.583
6→6a	1.228	1.097	1.515	1.087	0.306
6→6b	1.249	1.097	1.468	1.085	0.397
7→7a	1.232	1.096	1.509	1.087	0.322
7→7b	1.286	1.094	1.401	1.087	0.611
8→8a	1.224	1.097	1.520	1.089	0.295
8→8b	1.254	1.097	1.467	1.086	0.412
9→9a	1.231	1.098	1.503	1.088	0.320
9→9b	1.291	1.094	1.395	1.087	0.640
10→10a	1.238	1.099	1.482	1.087	0.352
10→10b	1.255	1.097	1.451	1.088	0.435
11→11a	1.227	1.098	1.501	1.089	0.313
11→11b	1.289	1.094	1.399	1.088	0.627
12→12a	1.24	1.098	1.482	1.088	0.360
12→12b	1.247	1.098	1.460	1.088	0.404

In these cases, 1,6-H shift is disfavored not only enthalpically but also entropically. The difference in activation entropy between six- and seven-membered ring transition states varies between 0.4−2.8 cal/mol/K, which corresponds to 0.12−0.83 kcal/mol at 298 K.

The situation is completely reversed in the valine series (radicals **10** and **12**), since the exergonicities of the two processes become similar. According to calculations, for these radicals 1,6-H shift should be favored and moreover be the only pathway, which is attested by the experimental results obtained from **1b**. By opposition to radicals **9** and **11**, in the cases of radicals **10** and **12**, 1,6-H shift is favored both enthalpically and entropically.

The reaction profiles and geometries of transition states for the competitive evolutions of radical **11** and **12** are given in Figures 3 and 4, respectively. Figure 4 gives clear evidence that the bulky substituent attached to nitrogen controls the preferred conformation of radical **12** and contributes to increase the activation free energy of 1,5-hydrogen shift.

The main differences in torsional interactions around C−N and C−S single bonds are illustrated in Figure 5. The simple examination of the main torsional angles accounts for the higher energy of the conformer predisposed to 1,5-H transfer.

Experimental Evidence for the Influence of *N*-Tosyl Group. In order to test the validity of the theoretical prediction, enediyne (±)-**13** was prepared from *N*-methylvaline methyl ester. The difficulties in preparing strictly the *N*-methyl analogue of **1b** led us to use the strategy recently devised using one-pot Crabbé homologation/tandem enynyne−allene (±)-**14** rearrangement.[6] The experimental results are reported in Scheme 2.

The one-pot multistep reaction led to a mixture of products (±)-**15** (28%) and (±)-**16** (25%), resulting from exclusive 1,5-H shift but from both the captodative position and the methyl group. Despite the reaction enthalpy is in favor of hydrogen

dx.doi.org/10.1021/jo202580y | J. Org. Chem. 2012, 77, 2773−2783

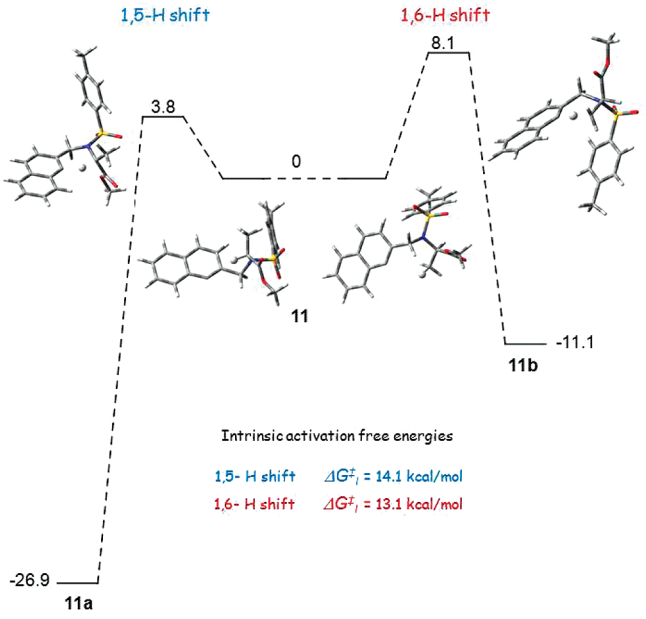

Figure 3. Competitive reaction pathways for the translocation of radical **11** (activation free energies and exergonicities in kcal/mol).

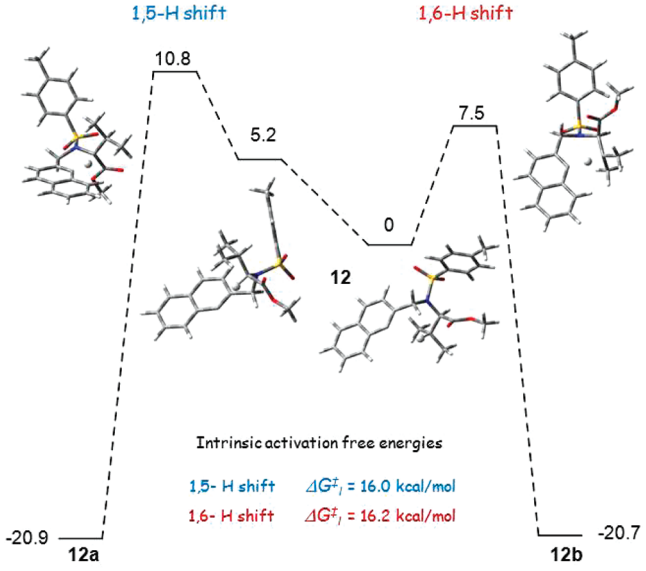

Figure 4. Competitive reaction pathways for the translocation of radical **12** (activation free energies and exergonicities in kcal/mol).

abstraction from the captodative position, hydrogen abstraction from the methyl group competes. It is enhanced by the statistic factor (3H/1H) and probably by steric effects. Side products resulting from oxidative degradation were detected in the crude mixture that could not be quantified nor identified. These data confirmed the dramatic incidence of the methyl group on the fate of diradical **D** the isolated products resulted from 1,5-H shift in agreement with theoretical predictions made for radical **8** (Chart 1, eqs 12 and 13, and Table 1). The additional incidence of the absence of substituent at the benzylic radical center, contributes to an important slowing down of the disproportionation pathway. No product resulting from disproportionation was isolated or detected in the crude mixture.[6]

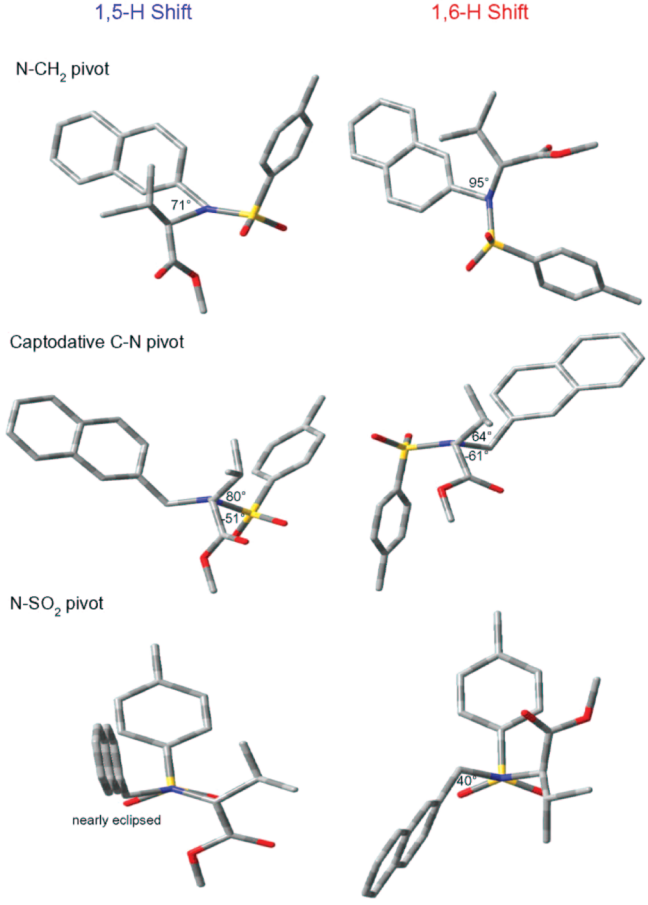

Figure 5. Compared torsional interactions around the two C−N and the C−S bonds in the two reactive conformers of radical **12** (on the left, views of the conformer predisposed for 1,5-H shift; on the right, views of the conformer predisposed to 1,6-H shift. Hydrogen atoms were removed for the sake of clarity).

Scheme 2. Tandem Crabbe Homologation/Rearrangement of (±)-13

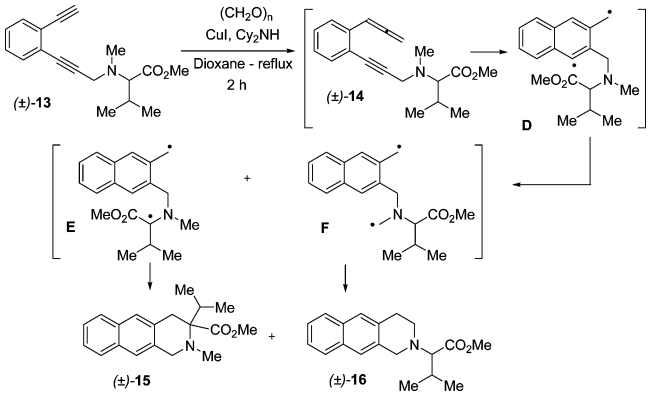

Cascade Rearrangements Leading to Naphthoazepines. The availability of tricyclic products resulting from 1,6-hydrogen shift should be reinforced by favorable enthalpic factors. Thus, in the absence of any competitive 1,5-H shift, the enantioselective synthesis of seven-membered ring cyclic amino esters bearing a quaternary stereogenic center was an obvious application of the methodology.

Homopropargylic aminoester (*S*)-**17** (85% ee) was prepared from (*S*)-*N*-tosylalanine methyl ester. Submitted to the action

dx.doi.org/10.1021/jo202580y | J. Org. Chem. 2012, 77, 2773−2783

Scheme 3. Cyclization of (*S*)-17

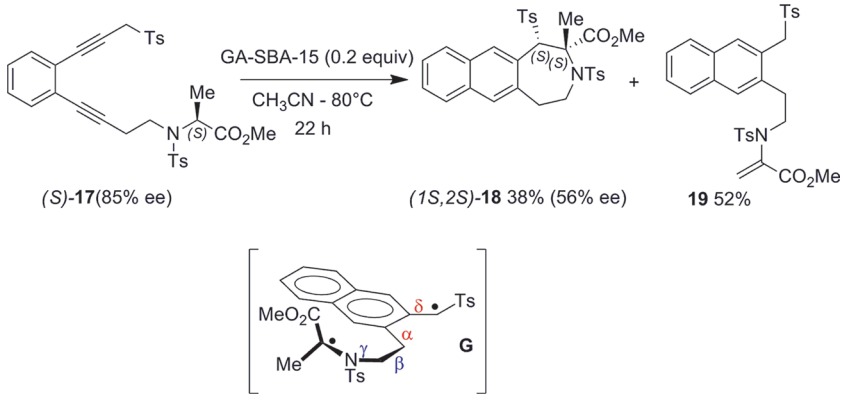

Scheme 4. Rearrangement of 4

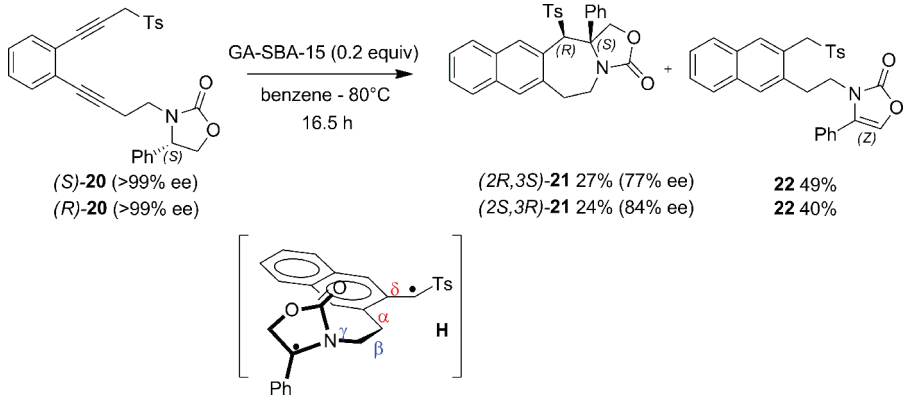

of GA-SBA-15, (*S*)-**17** led to (1*S*,2*S*)-**18** in 38% yield and 56% ee (Scheme 3).[28] The major product **19** resulted again from disproportionation.

In spite of the increased number of rotational degrees of freedom in the side chain bearing the reactive captodative center in biradical **G** and as this radical center (issued this time from 1,6-hydrogen transfer) was formed in a chiral conformation, memory of chirality was still observed. This means that recombination via rotation around the two single bonds adjacent to the aromatic system, i.e., bonds α and δ, remained the fastest pathway. Naphtho-azepine **18** was isolated as a single isomer in 56% ee.[29]

In order to suppress any competitive disproportionation, attempts to synthesize optically pure enediyne derived from phenyl glycine failed, and only the racemic starting material could be obtained (this is due to the acidity of the proton in the benzylic captodative position).

In order to overcome the increased acidity of the proton in the synthesis of the enediyne substrate, and at the same time to improve the level of memory of chirality by reducing the conformational flexibility, enediyne (*S*)- and (*R*)-**20** were prepared from the oxazolidinones derived from (*S*)- and (*R*)-phenyl glycinols, respectively. The results are shown in Scheme 4. Previous studies had shown that the tetracyclic sulfones derived from these oxazolidinones were easily epimerized in acetonitrile. Therefore, the rearrangement of **20** was achieved under different experimental conditions, and benzene was first selected as the most suitable solvent to minimize the possible epimerization of the cis and trans isomers of product **21**.[30]

Much to our disappointment, the increased flexibility of the side chain promoted a disproportionation, that is, hydrogen migration from the position α to oxygen in the oxazolidinone ring to the benzylic radical center leading to **22** in 40 or 49% yield. The reaction is enantioselective, oxazepin **21** was obtained as a single diastereomer in 24% yield and 84% ee from (*R*)-**20** and its enantiomer was isolated in 27% yield and 77% ee from (*S*)-**20**.[29]

The high ee provides an indirect proof that the rotations around the non benzylic C−C and C−N single bonds β and γ are still hindered as compared to rotation around bond α in diradical **H**. However, this investigation showed that the increased flexibility in the side chain enables disproportionation pathways that were not observed in experiments performed on the previous set of homologous propargylic substrates, undergoing the closure of six-membered rings in the last elementary step of the cascade rearrangement.[1] This is a severe limitation to the yield in enantio-enriched naphtoazepines that could be prepared according to this pathway.

■ CONCLUSION

In summary, the cascade rearrangement of enediynes of type **1**, starting with 1,3-proton shift immediately followed by Saito−Myers cyclization, was shown to evolve via exclusive 1,5- or 1,6-hydrogen shift depending on the structure of the starting material. Computational data confirmed these kinetic preferences. The dramatic influence of the substituent attached to the nitrogen atom of the amino ester moiety was emphasized. In the alanine derivative **1a**, exclusive 1,5-hydrogen abstraction of the hydrogen atom in captodative position is well accounted for by the incidence of the greater exergonicity of this process as compared to 1,6-hydrogen shift from the methyl group.

dx.doi.org/10.1021/jo202580y | *J. Org. Chem.* 2012, 77, 2773−2783

Conversely, the "exclusive" kinetic preference for 1,6-hydrogen abstraction over 1,5-migration of the hydrogen atom in captodative position, observed in the rearrangement of the valine derivative **1b**, is quite unexpected. It is the bulky tosyl group attached to nitrogen which contributes to increase the activation free energy of 1,5-hydrogen shift. This is rationalized, according to theoretical calculations, by the higher energy of the conformation that must be reached for model radical **12** to be ready to transfer the hydrogen atom from the captodative position. The validity of calculations was confirmed by the rearrangement of *rac*-enediyne **13**.

The ready occurrence of 1,6-hydrogen transfer was tentatively exploited, with compounds where no competitive 1,5-hydrogen shift is available, to achieve the enantioselective synthesis of naphthoazepines based on the phenomenon of memory of chirality. The main drawback is that, whenever possible without introducing torsional constraints, disproportionation becomes the major pathway with respect to recombination in the last elementary step.

EXPERIMENTAL SECTION

Rearrangement of (*S*)-1b. A solution of (*S*)-**1b** (95 mg, 0.16 mmol) and GA-SBA-15 (23 mg, 0.03 mmol) in CH_3CN (10 mL) was stirred for 18 h at 80 °C. Then the solvent was removed in vacuo, and the residue was purified by flash chromatography on silica gel (pentane/Et_2O, 90/10 to 50/50). This led to **4b** (63 mg, 66%) as a yellow oil.

Methyl (2*S*)-3-Methyl-2-{*N*-[(3-{[(4-methylbenzene)sulfonyl]-methyl}naphthalen-2-yl)methyl](4-methylbenzene)-sulfonamido}but-3-enoate (4b). ee > 99% (Chiralpak IA, hexane/EtOH 70/30, 1 mL/min, $t_R(R)$ = 11.44 min, $t_R(S)$ = 12.69 min, $k(R)$ = 2.81, $k(S)$ = 3.23, α = 1.15, R_S = 1.74). $[\alpha]^{25}_D$ +29 (*c* 1.7, $CHCl_3$). HRMS (ESI): *m*/*z* calcd for $[M + NH_4]^+$ $C_{32}H_{37}N_2O_6S_2$ 609.2088, found 609.2091. ^{1}H NMR (400 MHz, $CDCl_3$) δ: 7.92 (1H, s), 7.71−7.69 (1H, br d, *J* = 8.2), 7.64−7.62 (1H, br d, *J* = 7.5), 7.54 (2H, d, *J* = 8.0), 7.51 (2H, d, *J* = 8.0), 7.47−7.40 (2H, m), 7.39 (1H, s), 7.23 (2H, d, *J* = 8.0), 7.16 (2H, d, *J* = 8.0), 5.07 (1H, s), 4.81 (1H, s), 4.74 (1H, s), 4.66 (2H, s), 4.62 (1H, d (A part of AB pattern), *J* = 14.3), 4.55 (2H, d (B part of AB pattern), *J* = 14.3), 3.43 (3H, s), 2.43 (3H, s, CH_3), 2.36 (3H, s), 1.58 (3H). ^{13}C NMR (100 MHz, $CDCl_3$) δ: 170.0, 144.9, 143.7, 138.8, 136.7, 135.4, 134.2, 133.1, 132.2, 132.1, 129.9, 129.7 (2 × C), 129.4 (2 × C), 128.9 (2 × C), 127.8, 127.5, 127.4 (2 × C), 126.8, 126.4, 124.6, 117.4, 64.4, 60.0, 52.0, 46.3, 21.8, 21.6, 21.5.

Methyl 3-Methyl-2-{*N*-[(3-{[(4-methylbenzene)sulfonyl]-methyl}naphthalen-2-yl)methyl](4-methylbenzene)-sulfonamido}but-2-enoate (3b). A solution of (*S*)-**4b** (67 mg, 0.11 mmol) and GA-SBA-15 (160 mg, 0.23 mmol) in CH_3CN (7 mL) was stirred for 7 days at 80 °C. Then the mixture was filtered and washed with dichloromethane. The solvent was removed in vacuo, and the residue was purified by flash chromatography on silica gel (pentane/Et_2O, 80/20 to 40/60). This led to **3b** (47 mg, 70%) as a yellow oil. HRMS (ESI): *m*/*z* calcd for $[M + NH_4]^+$ $C_{32}H_{37}N_2O_6S_2$ 609.2088, found 609.2087. ^{1}H NMR (400 MHz, $CDCl_3$) δ: 7.89 (2H, d, *J* = 8.3), 7.79−7.69 (5H, m), 7.53−7.44 (2H, m), 7.39 (1H, s), 7.35 (4H, d, *J* = 8.0), 5.54 (1H, d, *J* = 13.8), 5.38 (1H, d, *J* = 13.8), 4.38 (1H, d, *J* = 13.5), 4.31 (1H, d, *J* = 13.8), 4.31 (3H, s), 2.47 (3H, s), 2.46 (3H, s), 1.87 (3H, s), 1.31 (3H, s). ^{13}C NMR (100 MHz, $CDCl_3$) δ: 164.9, 160.04, 144.9, 143.53, 136.6, 136.5, 133.3, 133.06, 133.00, 132.1, 132,0, 129,9 (2 × C), 129,5 (2 × C), 128.8 (2 × C), 128.0 (2 × C), 127.9, 127,6, 127.1, 126.9, 125.4, 121.4, 59.1, 51.1, 50.9, 23.8, 22.0, 21.8, 21.7.

Rearrangement of (*rac*)-*d1*-1a. A solution of (*rac*)-*d1*-**1a** (183 mg, 0.32 mmol) and GA-SBA-15 (46 mg, 0.06 mmol) in CH_3CN (18 mL) was stirred for 15 h at 80 °C. Then the solvent was removed in vacuo, and the residue was purified by flash chromatography on silica gel (dichloromethane/Et_2O, 100/00 to 99/1). This led to three products, (3*S**, 4*R**)-*d1*-**2a** (73 mg, 40%, 75% deuterium labeling), (3*S**, 4*S**)-*d1*-**2a** (63 mg, 35%, 81% deuterium labeling), and *d1*-**3a** (38 mg, 21%, 75% deuterium labeling).

Methyl (3*S,4*R**)-3-Methyl-2,4-bis[(4-methylbenzene)-sulfonyl](10-^{2}H)-1*H*,2*H*,3*H*,4*H*-benzo[*g*]isoquinoline-3-carboxylate (*d1*-2a).** HRMS (ESI): *m*/*z* calcd for $[M + NH_4]^+$ $C_{30}H_{32}DN_2O_6S_2$ 582.1837, found 582.1833. ^{1}H NMR (400 MHz, $CDCl_3$) δ: 7.85 (2H, d, *J* = 8.3), 7.73 (1H, br d, *J* = 8.8), 7.59 (1H, br d, *J* = 7.8), 7.50−7.40 (2.25H, dt (2H) plus superimposed residual s (0.25H)), 7.33−7.26 (5H, m (s superimposed to two d)), 7.08 (2H, d, *J* = 7.9), 4.89 (1H, d, *J* = 15.3, A part of an AB pattern), 4.73 (1H, s), 4.63 (1H, d, *J* = 15.1, B part of an AB pattern), 3.15 (3H, s), 2.42 (3H, s), 2.39 (3H, s), 2.34 (3H, s). ^{2}H NMR (61.4 MHz, acetone) δ: 7.73 (br s).

Methyl (3*S,4*S**)-3-Methyl-2,4-bis[(4-methylbenzene)-sulfonyl](10-^{2}H)-1*H*,2*H*,3*H*,4*H*-benzo[*g*]isoquinoline-3-carboxylate (*d1*-2a).** HRMS (ESI): *m*/*z* calcd for $[M + NH_4]^+$ $C_{30}H_{32}DN_2O_6S_2$ 582.1837, found 582.1835. ^{1}H NMR (400 MHz, $CDCl_3$) δ: 7.99 (2H, d, *J* = 8.3), 7.77 (1H, d, *J* = 7.9), 7.57 (0.19H, s, residual CH_{ar}), 7.54−7.46 (1H, m), 7.43 (2H, m), 7.33 (1H, d, *J* = 8.1), 7.36−7.29 (1H, m), 7.25 (2H, d, *J* = 8.1), 7.00 (2H, d, *J* = 8.1), 6.86 (1H, s), 4.60 (2H, br s), 4.50 (1H, s), 4.01 (3H, s), 2.44 (3H, s), 2.33 (3H, s), 1.76 (3H, s). ^{2}H NMR (61.4 MHz, acetone) δ: 7.85 (br s).

Methyl 2-{*N*-[(3-{[(4-Methylbenzene)sulfonyl](^{2}H$_1$)methyl}-naphthalen-2-yl)methyl](4-methylbenzene)sulfonamido}(^{2}H$_2$)-prop-2-enoate (*d1*-3a). HRMS (ESI): *m*/*z* calcd for $[M + NH_4]^+$ $C_{30}H_{32}DN_2O_6S_2$ 582.1837, found 582.1840. ^{1}H NMR (400 MHz, $CDCl_3$) δ: 7.88 (2H, d, *J* = 8.3), 7.77 (1H, s), 7.74 (2H, d, *J* = 8.3), 7.79−7.64 (2H, superimposed m), 7.50−7.44 (2H, m), 7.43 (0.25H, residual s), 7.37−7.32 (4H, 2 × d, *J* = 8.1), 6.14 (1H, s), 5.44 (1H, s), 4.84 (2H, s), 4.77 (2H, s), 3.53 (3H, s), 2.48 (3H, s), 2.47 (3H, s). ^{2}H NMR (61.4 MHz, acetone) δ: 7.75 (br s).

Rearrangement of (*rac*)-*d1*-1b. Monodeuterated (rac)-*d1*-**4b** was prepared according to the procedure already described for the synthesis of **4b**, using (rac)-*d1*-**1b** (101 mg, 0.17 mmol) and GA-SBA-15 (24 mg, 0.03 mmol) in CH_3CN (10 mL). The reaction mixture was stirred for 18 h at 80 °C. After workup, purification by liquid chromatography on silica gel (pentane/Et_2O, 70/30 to 60/40) led to (*rac*)-*d1*-**4b** (66 mg, 65% yield, and 83% deuterium labeling) as a yellow oil.

(*rac*)-Methyl 3-methyl-2-{*N*-[(3-{[(4-methylbenzene)-sulfonyl]methyl}naphthalen-2-yl)methyl](4-methylbenzene)-sulfonamido}(2-^{2}H)but-3-enoate (*d1*-4b). HRMS (ESI): *m*/*z* calcd for $[M + NH_4]^+$ $C_{32}H_{36}DN_2O_6S_2$ 610.2150, found 610.2136. ^{1}H NMR (400 MHz, $CDCl_3$) δ: 7.92 (1H, s), 7.71−7.69 (1H, m), 7.64−7.62 (1H, m), 7.53 (2H, d, *J* = 8.3), 7.51 (2H, d, *J* = 8.3), 7.47−7.40 (2H, m), 7.39 (1H, s), 7.23 (2H, d, *J* = 8.0), 7.16 (2H, d, *J* = 8.0), 5.07 (0.16H, residual s), 4.81 (1H, s), 4.74 (1H, s), 4.66 (2H, s), 4.62 (1H, d (A part of AB pattern), *J* = 14.3), 4.55 (2H, d (B part of AB pattern), *J* = 14.3), 3.43 (3H, s), 2.43 (3H, s), 2.36 (3H, s), 1.58 (3H, s). ^{2}H NMR (61.4 MHz, acetone) δ: 5.08 (br s).

Rearrangement of (*rac*)-*d3*-1a. A solution of (*rac*)-*d3*-**1a** (200 mg, 0.35 mmol) and GA-SBA-15 (50 mg, 0.07 mmol) in CH_3CN (20 mL) was stirred for 15 h at 80 °C. Then the solvent was removed in vacuo, and the residue was purified by flash chromatography on silica gel (pentane/dichloromethane, 50/50 to 80/20). This led to three products, (3*S**,4*R**)-*d3*-**2a** (90 mg, 45%, 100% deuterium labeling), (3*S**,4*S**)-*d3*-**2a** (77 mg, 38%, 100% deuterium labeling), and *d3*-**3a** (20 mg, 10%, 100% deuterium labeling).

Methyl (3*S*,4*R*)-3-(^{2}H$_3$)Methyl-2,4-bis[(4-methylbenzene)-sulfonyl]-1*H*,2*H*,3*H*,4*H*-benzo[*g*]isoquinoline-3-carboxylate (*d3*-2a). HRMS (ESI): *m*/*z* calcd for $[M + NH_4]^+$ $C_{30}H_{30}D_3N_2O_6S_2$ 584.1963, found 584.1958. ^{1}H NMR (400 MHz, $CDCl_3$) δ: 7.87 (2H, d, *J* = 8.3), 7.75 (1H, br d, *J* = 7.9), 7.61 (1H, br d, *J* = 7.6), 7.50 (1H, s), 7.50−7.40 (2H, m), 7.33−7.26 (5H, m (s superimposed to two d)), 7.08 (2H, d, *J* = 7.9), 4.91 (1H, d, *J* = 15.3, A part of an AB pattern), 4.74 (1H, s), 4.63 (1H, d, *J* = 15.1, B part of an AB pattern), 3.17 (3H, s), 2.40 (3H, s), 2.37 (3H, s). ^{2}H NMR (61.4 MHz, acetone) δ 2.34 (br s).

Methyl (3*S*,4*S*)-3-(^{2}H$_3$)Methyl-2,4-bis[(4-methylbenzene)-sulfonyl]-1*H*,2*H*,3*H*,4*H*-benzo[*g*]isoquinoline-3-carboxylate

dx.doi.org/10.1021/jo202580y | J. Org. Chem. 2012, 77, 2773−2783

(*d3*-2a). HRMS (ESI): *m*/*z* calcd for $[M + NH_4]^+$ $C_{30}H_{30}D_3N_2O_6S_2$ 584.1963, found 584.1958. ^{1}H NMR (400 MHz, $CDCl_3$) δ: 7.99 (2H, d, *J* = 8.3), 7.77 (1H, d, *J* = 7.9), 7.57 (1H, s), 7.54−7.46 (1H, m), 7.45−7.40 (2H, m), 7.33 (2H, d, *J* = 8.1), 7.25 (2H, d, *J* = 8.3), 7.00 (2H, d, *J* = 8.1), 6.87 (1H, s), 4.60 (2H, br s), 4.50 (1H, s), 4.01 (3H, s), 2.44 (3H, s), 2.33 (3H, s). ^{2}H NMR (61.4 MHz, acetone) δ 1.67 (br s).

Methyl 2-{*N*-[(3-{[(4-Methylbenzene)sulfonyl]($^2H_1$)methyl}-naphthalen-2-yl)methyl](4-methylbenzene)sulfonamido}($^2H_2$)-prop-2-enoate (*d3*-3a). HRMS (ESI): *m*/*z* calcd for $[M + NH_4]^+$ $C_{30}H_{30}D_3N_2O_6S_2$ 584.1963, found 584.1961. ^{1}H NMR (400 MHz, $CDCl_3$) δ: 7.88 (2H, d, *J* = 8.3), 7.77 (1H, s), 7.77−7.72 (3H, superimposed m), 7.69−7.64 (1H, m), 7.52−7.45 (2H, m), 7.43 (1H, s), 7.37−7.32 (4H, 2 superimposed d, *J* = 8.1), 4.84 (1H, s), 4.77 (2H, s), 3.53 (3H, s), 2.48 (3H, s), 2.47 (3H, s). ^{2}H NMR (61.4 MHz, acetone) δ: 6.15 (br s), 5.63 (br s), 5.00 (br s).

Rearrangement of (±)-13. $(CH_2O)_n$ (26 mg, 0.88 mmol), CuI (34 mg, 0.18 mmol), 1,4-dioxane (1 mL), enediyne (±)-**13** (100 mg, 0.35 mmol), and dicylohexylamine (115 mg, 0.63 mmol) were added sequentially into a flask equipped with a reflux condenser under an argon atmosphere. The resulting mixture was stirred at reflux for 2 h. Solvent was evaporated under vacuo, the residue was dissolved in DCM and filtered over a short pad of Celite, and the filtrate was concentrated and purified by column chromatography on silica gel using pentane/Et_2O (95:5 to 90:10) as eluent to afford (±)-**15** (29 mg, 28%) and (±)-**16** (26 mg, 25%).

Methyl 2-Methyl-3-(propan-2-yl)-1*H*,2*H*,3*H*,4*H*-benzo[*g*]-isoquinoline-3-carboxylate (±)-15. HRMS (ESI): *m*/*z* calcd for $[M + H]^+$ $C_{19}H_{24}NO_2$ 298.1802, found 298.1801. ^{1}H NMR (400 MHz, $CDCl_3$) δ: 7.75−7.69 (2H, m), 7.62 (1H, s), 7.46 (1H, s), 7.40−7.33 (2H, m), 4.10 (1H, d (A part of AB pattern), *J*= 16.3), 3.77 (1H, d (B part of AB pattern), *J* = 16.3), 3.60 (3H, s), 3.31 (1H, d (A part of AB pattern), *J* = 16.3), 3.02 (1H, d (B part of AB pattern), *J* = 16.3), 2.58 (3H, s), 2.45 (1H, sept, *J* = 6.8), 1.06 (3H, d, *J* = 6.8), 1.00 (3H, d, *J* = 6.8). ^{13}C NMR (100 MHz, $CDCl_3$) δ: 173.8, 133.0, 132.6, 132.2, 132.0, 127.3, 127.2, 126.5, 125.2, 125.1, 124.0, 68.6, 55.3, 51.1, 38.2, 31.3, 29.8, 18.0, 16.6.

Methyl 2-{1*H*,2*H*,3*H*,4*H*-Benzo[*g*]isoquinolin-2-yl}-3-methylbutanoate (±)-16. HRMS (ESI): *m*/*z* calcd for $[M + H]^+$ $C_{19}H_{24}NO_2$ 298.1802, found 298.1803. ^{1}H NMR (400 MHz, $CDCl_3$) δ: 7.74−7.69 (2H, m), 7.57 (1H, s), 7.50 (1H, s), 7.40−7.35 (2H, m), 4.00−3.90. (2H, AB pattern, J_{AB} = 16.3), 3.73 (3H, s), 3.10−3.02 (3H, m), 3.01 (1H, d, *J* = 10.8), 2.79 (1H, m), 2.27−2.16 (1H, m), 1.03 (3H, d, *J* = 6.8), 0.95 (3H, d, *J* = 6.8). ^{13}C NMR (100 MHz, $CDCl_3$) δ: 172.3, 134.2, 133.6, 132.4, 132.0, 127.3, 127.2, 126.8, 125.3, 125.3, 124.6, 74.4, 53.3, 50.8, 47.2, 30.4, 27.3, 20.0, 19.5.

Rearrangement of (*S*)-17. Compound (*S*)-**17** (100 mg, 0.17 mmol) and GA-SBA-15 (24 mg, 0.03 mmol) were dissolved in CH_3CN (10 mL). The mixture was heated at 80 °C for 22 h. Then the solvent was removed in vacuo, and the residue was purified by flash chromatography on silica gel (pentane/dichloromethane, 50/50 to 0/100). This led to (1*S*, 2*S*)-**18** (38 mg, 38%) as a yellow oil and **19** (52 mg, 52%) as a yellow oil.

Methyl (1*S*,2*S*)-2-Methyl-1,3-bis[(4-methylbenzene)-sulfonyl]-1*H*,2*H*,3*H*,4*H*,5*H*-naphtho[2,3-*d*]azepine-2-carboxylate (18). ee = 56% (Chiralpak IC, hexane/EtOH 50/50, 1 mL/min, t_R(1*S*,2*S*) = 15.80 min, t_R(1*S*,2*S*) = 28.43 min, *k*(1*R*,2*R*) = 4.27, *k*(1*R*,2*S*) = 8.45, α = 1.98, R_S = 7.05). $[\alpha]^{25}_D$ +23 (*c* 0.6, $CHCl_3$). HRMS (ESI): *m*/*z* calcd for $[M + NH_4]^+$ $C_{31}H_{35}N_2O_6S_2$ 595.1931, found 595.1928. ^{1}H NMR (400 MHz, $CDCl_3$) δ: 7.73 (1H, d, *J* = 8.0), 7.62 (1H, s), 7.47 (2H, d, *J* = 8.3), 7.41 (1H, dt, J= 1.0 and 6.8), 7.33−7.29 (3H, m), 7.22 (1H, d, *J* = 8.0), 7.11 (2H, d, *J* = 8.0), 7.05 (2H, d, *J* = 8.0), 6.68 (1H, s), 5.95 (1H, s), 4.11 (1H, ddd, *J* = 6.8, 11.8 and 14.8), 3.92−3.80 (2H, m), 3.62 (3H, s), 3.00 (1H, ddd, *J* = 1.8, 5.3 and 14.8), 2.55 (3H, s), 2.35 (3H, s), 2.32 (3H, s). ^{13}C NMR (100 MHz, $CDCl_3$) δ 172.5, 145.7, 142.8, 139.3, 136.2, 135.9, 135.7, 133.7, 131.7, 129.3, 129.3 (2 × C), 129.22 (2 × C), 129.21 (2 × C), 129.0, 127.7, 127.1, 126.8, 126.4 (2 × C), 125.7, 78.4, 66.6, 53.4, 45.4, 33.0, 23.3, 21.6, 21.5. The *cis* stereochemistry was assigned from 2D NMR experiments. The NOESY spectrum shows a clear cross-peak between the signal of the proton at 5. 95 ppm and the signal of the methyl protons at 2.55 ppm.

Methyl 2-{*N*-[2-(3-{[(4-Methylbenzene)sulfonyl]methyl}-naphthalen-2-yl)ethyl](4-methylbenzene)sulfonamido}prop-2-enoate (19). HRMS (ESI): *m*/*z* calcd for $[M + NH_4]^+$ $C_{31}H_{35}N_2O_6S_2$ 595.1931, found 595.1928. ^{1}H NMR (400 MHz, $CDCl_3$) δ: 7.73 (1H, d, *J* = 8.0), 7.69−7.66 (1H, m), 7.68 (1H, superimposed s), 7.66 (1H, superimposed s, CH_{ar}), 7.62 (2H, d, *J* = 8.5), 7.59 (2H, d, *J* = 8.5), 7.50−7.41 (2H, m), 7.26 (2H, d, *J* = 8.0), 7.23 (2H, d, *J* = 8.0), 6.44 (1H, s), 5.81 (1H, s), 4.49 (2H, br s), 3.65 (3H, s), 3.64−3.60 (2H, m), 2.97−2.93 (2H, m), 2.43 (3H, s), 2.43 (3H, s). ^{13}C NMR (100 MHz, $CDCl_3$) δ: 164.3, 145.0, 143.8, 136.0, 135.7, 135.2, 133.5, 132.6, 132.1, 129.8 (2 × C), 129.6 (2 × C), 129.2, 128.8, 128.7 (2 × C), 127.8 (2 × C), 127.7, 127.2, 127.0, 126.2, 124.8, 59.6, 52.6, 50.3, 32.5, 21.8, 21.7. One carbon is missing probably due to overlapping.

Rearrangement of (*R*)-20. (*R*)-**20** (100 mg, 0.21 mmol) and GA-SBA-15 (29 mg, 0.04 mmol) were dissolved in benzene (10 mL). The mixture was heated at 80 °C for 16.5 h. The solvent was removed in vacuo, and the residue was purified by flash chromatography on silica gel (pentane/AcOEt, 80/20 to 50/50). This led to (2*S*,3*R*)-**21** (24 mg, 24%) as a yellow amorphous solid and **22** (40 mg, 40%) as a yellow amorphous solid.

(2*S*,3*R*)-2-[(4-Methylbenzene)sulfonyl]-3-phenyl-5-oxa-7-azatetracyclo[8.8.0.0^{3,7}.0^{12,17}]octadeca-1(18),10,12(17),13,15-pentaen-6-one (21). ee = 84% (Chiralpak IB, hexane/EtOH/chloroform 60/30/10, 1 mL/min, t_R(2*S*, 3*R*) = 6.56 min, t_R(2*R*, 3*S*) = 8.21 min, *k*(2*S*,3*R*) = 1.19, *k*(2*R*,3*S*) = 1.68, α = 1.41 and R_S = 2.70). $[\alpha]^{25}_D$ −103 (*c* 0.48, $CHCl_3$). HRMS (ESI): *m*/*z* calcd for $[M + NH_4]^+$ $C_{29}H_{29}N_2O_4S$ 501.1843, found 501.1842. ^{1}H NMR (400 MHz, $CDCl_3$) δ: 7.59 (1H, d, *J* = 8.0), 7.43−7.23 (10H, m), 7.15 (1H, tt, *J* = 8.3 and 1.5), 6.98 (1H, s), 6.91 (2H, d, *J* = 8.0), 5.72 (1H, d, *J* = 9.0), 5.19 (1H, s), 4.40 (1H, ddd, *J* = 14.3, 7.3 and 2.8), 4.25 (1H, br t, *J* = 14.0), 4.07 (1H, d, *J* = 9.0), 3.26 (1H, pseudo t, *J* = 13.0), 2.80 (1H, br dd, *J* = 15.3 and 4.0), 2.12 (3H, s). ^{13}C NMR (100 MHz, $CDCl_3$) δ: 158.2, 144.9, 140.0, 138.1, 136.4, 135.8, 132.8, 131.4, 130.0, 129.5 (2 × C), 129.2 (2 × C), 128.8, 128.5 (2 × C), 128.3, 127.3, 127.0, 126.9, 126.1, 125.9 (2 × C), 77.8, 74.0, 67.7, 40.9, 35.8, 21.4. In full agreement with the Chem-3D model showing a π-stacking interaction, the stereochemistry was assigned from 2D NMR experiments. The NOESY spectrum shows a clear cross-peaks between the signal of the proton in position α to the tosyl group at 5.19 ppm and the s signal of one aromatic proton of the naphthyl group at 6.98 ppm and the d of one proton of the CH_2O group of the carbamate ring at 5.72 ppm.

3-[2-(3-{[(4-Methylbenzene)sulfonyl]methyl}naphthalen-2-yl)ethyl]-4-phenyl-2,3-dihydro-1,3-oxazol-2-one (22). HRMS (ESI): *m*/*z* calcd for $[M + NH_4]^+$ $C_{29}H_{29}N_2O_4S$ 501.1843, found 501.1840. ^{1}H NMR (400 MHz, $CDCl_3$) δ: 7.69−7.65 (2H, m), 7.54 (2H, d, *J* = 8.3), 7.51 (1H, s), 7.49−7.37 (6H, m), 7.23 (2H, d, *J* = 8.3), 7.13−7.09 (2H, m), 6.74 (1H, s), 4.28 (2H, s), 3.82−3.77 (2H, m), 2.96−2.91 (2H, m), 2.42 (3H, s). ^{13}C NMR (100 MHz, $CDCl_3$) δ: 156.1, 145.0, 135.5, 134.5, 133.5, 132.8, 132.2, 129.9, 129.8 (2 × C), 129.7, 129.4, 129.3 (2 × C), 128.8 (2 × C), 128.6 (2 × C), 127.8, 127.2, 127.1, 126.3, 126.3, 124.7, 123.9, 59.3, 43.0, 31.8, 21.8.

Rearrangement of (*S*)-20. (*S*)-**20** (200 mg, 0.41 mmol) and GA-SBA-15 (58 mg, 0.08 mmol) were dissolved in benzene (20 mL). The mixture was heated at 80 °C for 16.5 h. The solvent was removed in vacuo, and the residue was purified by flash chromatography on silica gel (pentane/AcOEt, 80/20 to 50/50). This led to (2*R*,3*S*)-**21** (54 mg, 27%) as a yellow amorphous solid and **22** (98 mg, 49%) as a yellow amorphous solid.

(2*R*,3*S*)-2-[(4-Methylbenzene)sulfonyl]-3-phenyl-5-oxa-7-azatetracyclo[8.8.0.0^{3,7}.0^{12,17}]octadeca-1(18),10,12(17),13,15-pentaen-6-one (21). ee = 77% (Chiralpak IB, hexane/EtOH/chloroform 60/30/10, 1 mL/min, t_R(2*S*,3*R*) = 6.56 min, t_R(2*R*,3*S*) = 8.21 min, *k*(2*S*,3*R*)= 1.19, *k*(2*R*,3*S*) = 1.68, α = 1.41 and R_S = 2.70). $[\alpha]^{25}_D$ +118 (*c* 0.45, $CHCl_3$).

dx.doi.org/10.1021/jo202580y | *J. Org. Chem.* 2012, 77, 2773−2783

■ ASSOCIATED CONTENT

Supporting Information

Synthesis of starting materials, HPLC analyses, NMR spectra for all new compounds, and computational details. This material is available free of charge via the Internet at http://pubs.acs.org

■ AUTHOR INFORMATION

Corresponding Authors

*(A.G-S.) E-mail: anouk.siri@univ-cezanne.fr.
*(M.N.) E-mail: malek.nechab@univ-provence.fr.
*(M.P.B.) E-mail: michele.bertrand@univ-cezanne.fr.

Notes

The authors declare no competing financial interest.

■ ACKNOWLEDGMENTS

We thank the ANR (JCJC MOCER2) for financial support and the Université de Provence for the postdoctoral grant of Dr S. Mondal. This work was also supported by the computing facilities of the CRCMM.

■ REFERENCES

(1) Nechab, M.; Campolo, D.; Maury, J.; Perfetti, P.; Vanthuyne, N.; Siri, D.; Bertrand, M. P. *J. Am. Chem. Soc.* **2010**, *132*, 14742−14744.

(2) For selected examples of other cascade rearrangements of enediynes, following on from Bergman or Saito−Myers cyclizations, see: (a) Grissom, J. W.; Klingberg, D.; Huang, D.; Slattery, B. J. *J. Org. Chem.* **1997**, *62*, 603−626 and references therein. (b) Li, H.; Petersen, J. L.; Wang, K. K. *J. Org. Chem.* **2003**, *68*, 5512−5518. (c) Tarli, A.; Wang, K. K. *J. Org. Chem.* **1997**, *62*, 8841−8847. (d) Wang, K. K.; Wang, Z.; Tarli, A.; Gannett, P. *J. Am. Chem. Soc.* **1996**, *118*, 10783−10791. (e) Wang, K. K.; Zhang, H.-R.; Petersen, J. L. *J. Org. Chem.* **1999**, *64*, 1650−1656.

(3) (a) Fuji, K.; Kawabata, T. *Chem.—Eur. J.* **1998**, *4*, 373−376. (b) Zhao, H.; Hsu, D. C.; Carlier, P. R. *Synthesis* **2005**, 1−16. (c) Kawabata, T.; Fuji, K. In *Topics in Stereochemistry*; Denmark, S. E., Ed.; Wiley and Sons, Inc.; New York, 2003; Vol. *23*, pp 175−205.

(4) For examples of disproportionation of biradicals, see: (a) Bucher, G.; Mahajan, A. A.; Schmittel, M. *J. Org. Chem.* **2009**, *74*, 5850−5860. (b) Choe, T.; Khan, S. I.; Garcia-Garibay, M. A. *Photochem. Photobiol. Sci.* **2006**, *5*, 449−451. (c) Wagner, P. J.; Laidig, G. *Tetrahedron Lett.* **1991**, *32*, 895−898. (d) Wagner, P. J.; Chiu, C. *J. Am. Chem. Soc.* **1979**, *101*, 7134−7135.

(5) Nechab, M.; Besson, E.; Campolo, D.; Perfetti, P.; Vanthuyne, N.; Bloch, E.; Denoyel, R.; Bertrand, M. P. *Chem. Commun.* **2011**, *47*, 5286−5288.

(6) Mondal, S.; Nechab, M.; Vanthuyne, N.; Bertrand, M. P. *Chem. Commun.* **2012**, *48*, 2549−2551.

(7) For (3*S**,4*S**)-*d1*-**2a** the deuterated position gives rise to a residual s at 7.57 ppm (0.19H)/CHTs s at 4.50 ppm (1H). For (3*S**,4*R**)-*d1*-**2a** the deuterated position gives rise to a residual s superimposed to a m between 7.51 and 7.59 ppm (2.25H)/CHTs s at 4.72 ppm (1H). For *d1*-**3a** the deuterated position gives rise to a residual s at 7.43 ppm (0.25H)/=CH at 6.14 (1H) and 5.41 (1H), respectively.

(8) For the competitive migration of H/D in Schmittel rearrangement, see: Bucher, G.; Mahajan, A. A.; Schmittel, M. *J. Org. Chem.* **2009**, *74*, 5950−5860.

(9) For reviews, see: (a) Cekovic, Z. *J. Serb. Chem. Soc.* **2005**, *70*, 287−318. (b) Cekovic, Z. *Tetrahedron* **2003**, *59*, 8073. (c) Feray, L.; Kuznetsov, N.; Renaud, P. In *Radicals in Organic Synthesis*; Renaud, P., Sibi, M. P., Eds.; Wiley-VCH: Weinheim, 1998; Vol. *2*, pp 246−278. (d) Togo, H. In *Avanced Free Radical Reactions for Organic Synthesis*; Elsevier: Oxford, 2004; pp 171−186.

(10) (a) Dénès, F.; Beaufils, F.; Renaud, P. *Synlett* **2008**, 2389−2399. (b) Renaud, P.; Beaufils, F; Dénès, Feray, L.; Imboden, C.; Kuznetsov, N. *Chimia* **2008**, *62*, 510−513. (c) Robertson, J.; Pillai, J.; Lush, R. K. *Chem. Soc. Rev.* **2001**, *30*, 94−103.

(11) For examples of exclusive 1,6-hydrogen shift without possible competition of 1,5-hydrogen shift, see: (a) Gramain, J.-C.; Remuson, R.; Vallée, D. *J. Org. Chem.* **1985**, *50*, 710−712. (b) Furata, K.; Nagata, T.; Yamamoto, H. *Tetrahedron Lett.* **1988**, *29*, 2215−2218. (c) Kraus, G. A.; Chen, L. *J. Am. Chem. Soc.* **1990**, *112*, 3464−3466. (d) Bosch, E.; Bachi, M. D. *J. Org. Chem.* **1993**, *58*, 5581−5582. (e) Bogen, S.; Fensterbank, L.; Malacria, M. *J. Am. Chem. Soc.* **1997**, *119*, 5037−5038. (f) Manabe, T.; Yanagi, S.-I.; Ohe, K.; Uemura, S. *Organometallics* **1998**, *17*, 2942−2944. (g) Lin, H.; Schall, A.; Reiser, O. *Synlett* **2005**, 2603−2606. (h) Sakaguchi, N.; Hirano, S.; Matsuda, A.; Shuto, S. *Org. Lett.* **2006**, *8*, 3291−3294. (i) Yoshimura, Y.; Yamazaki, Y.; Wachi, K.; Satoh, S.; Takahata, H. *Synlett* **2007**, 111−114.

(12) For competitive processes, see: (a) Ayer, W. A.; Law, D. A.; Piers, K. *Tetrahedron Lett.* **1964**, *5*, 2959−2963. (b) José, I. C.; Francisco, C. G.; Hernández, R.; Salazar, J. A.; Suárez, E. *Tetrahedron Lett.* **1984**, *25*, 1953−1956. (c) McDonald, C. E.; Beebe, T.; Beard, M.; McMillen, D.; Selski, D. *Tetrahedron Lett.* **1989**, *30*, 4791−4794. (d) Bogen, S.; Fensterbank, L.; Malacria, M. *J. Org. Chem.* **1999**, *64*, 819−825. (e) Wille, U. *Chem.—Eur. J.* **2002**, *8*, 340−347. (f) Wille, U. *J. Am. Chem. Soc.* **2002**, *124*, 14−15. (g) Wille, U.; Heuger, G.; Jargstorff, C. *J. Org. Chem.* **2008**, *73*, 1413−1421 and previous references cited therein. (h) Harrowen, D. C.; Stenning, K. J.; Whiting, S.; Thompson, T.; Walton, R. *Org. Biomol. Chem.* **2011**, *9*, 4882−4885. (i) Francisco, C. G.; Freire, R.; Herrere, A. J.; Pérez-Martín, I.; Suárez, E. *Tetrahedron* **2007**, *63*, 8910−8920.

(13) (a) Curran, D. P.; Kim, D.; Liu, H. T.; Shen, W. *J. Am. Chem. Soc.* **1988**, *110*, 5900−5902. (b) Snieckus, V.; Cuevas, J.-C.; Sloan, C. P.; Liu, H.; Curran, D. P. *J. Am. Chem. Soc.* **1990**, *112*, 896−898. (c) Curran, D. P.; Somayajula, K. V.; Yu, H. *Tetrahedron Lett.* **1992**, *33*, 2295−2298. (d) Curran, D. P.; Shen, W. *J. Am. Chem. Soc.* **1993**, *115*, 6051−6059. (e) Yamasaki, N.; Eichenberger, E.; Curran, D. P. *Tetrahedron Lett.* **1994**, *35*, 6623−6226. (f) Curran, D. P.; Xu, J. Y. *J. Am. Chem. Soc.* **1996**, *118*, 3142−3147. (g) Curran, D. P.; Liu, W.; Chen, C. H.-T. *J. Am. Chem. Soc.* **1999**, *121*, 11012−11013.

(14) (a) Denenmark, D.; Hoffmann, P.; Winkler, T.; Waldner, A.; De Mesmaeker, A. *Synlett* **1991**, 621−624. (b) Denenmark, D.; Winkler, T.; Waldner, A.; De Mesmaeker, A. *Tetrahedron Lett.* **1992**, *33*, 621−624.

(15) (a) Dorigo, A. E.; Houk, K. N. *J. Am. Chem. Soc.* **1987**, *109*, 2195−2197. Conversely, in Norrish II photochemical reactions, 1,5-hydrogen transfer would be favored over 1−6 hydrogen migration by both enthalpic and entropic factors, see: (b) Dorigo, A. E.; McCarrick, M. A.; Loncharic, R. J.; Houk, K. N. *J. Am. Chem. Soc.* **1990**, *112*, 7508−7514.

(16) Rey, V.; Pierini, A.; Peñéñory, A. B. *J. Org. Chem.* **2009**, *74*, 1223−1230.

(17) For calculations of 1,5-H migration following on from a Bergman rearrangement, see: Baroudi, A.; Mauldin, J.; Alabugin, I. V. *J. Am. Chem. Soc.* **2010**, *132*, 967−979.

(18) Zeng, L.; Kaoudi, T.; Schiesser, C. H. *Tetrahedron Lett.* **2006**, *47*, 7911−7914.

(19) It can be noted that the presence of a nitrogen atom protected as an acetamide or a trifluoroacetamide in the chain makes the enthalpically favored 1,7-H migration of a benzylic hydrogen atom compete with 1,5-hydrogen shift.

(20) Gaussian 09, Revision A.02: Frisch, M. J.; Trucks, G. W.; Schlegel, H. B.; Scuseria, G. E.; Robb, M. A.; Cheeseman, J. R.; Scalmani, G.; Barone, V.; Mennucci, B.; Petersson, G. A.; Nakatsuji, H.; Caricato, M.; Li, X.; Hratchian, H. P.; Izmaylov, A. F.; Bloino, J.; Zheng, G.; Sonnenberg, J. L.; Hada, M.; Ehara, M.; Toyota, K.; Fukuda, R.; Hasegawa, J.; Ishida, M.; Nakajima, T.; Honda, Y.; Kitao, O.; Nakai, H.; Vreven, T.; Montgomery, J. A., Jr.; Peralta, J. E.; Ogliaro, F.; Bearpark, M.; Heyd, J. J.; Brothers, E.; Kudin, K. N.; Staroverov, V. N.; Kobayashi, R.; Normand, J.; Raghavachari, K.; Rendell, A.; Burant, J. C.; Iyengar, S. S.; Tomasi, J.; Cossi, M.; Rega, N.; Millam, N. J.; Klene, M.; Knox, J. E.; Cross, J. B.; Bakken, V.; Adamo, C.; Jaramillo, J.; Gomperts, R.; Stratmann, R. E.; Yazyev, O.;

Austin, A. J.; Cammi, R.; Pomelli, C.; Ochterski, J. W.; Martin, R. L.; Morokuma, K.; Zakrzewski, V. G.; Voth, G. A.; Salvador, P.; Dannenberg, J. J.; Dapprich, S.; Daniels, A. D.; Farkas, Ö.; Foresman, J. B.; Ortiz, J. V.; Cioslowski, J.; Fox, D. J. Gaussian, Inc., Wallingford, CT, 2009.

(21) Scott, A. P.; Radom, L. *J. Phys. Chem.* **1996**, *100*, 16502−16513.

(22) (a) Henry, D.; Sullivan, M.; Radom, L. *J. Chem. Phys.* **2003**, *118*, 4849−4860.

(23) Viehe, H. G.; Janousek, Z.; Merenyi, R.; Stella, L. *Acc. Chem. Res.* **1985**, *18*, 148−154.

(24) For recent discussions on radical stabilization energies, see: (a) Coote, M. L.; Lin, C. Y.; Beckwith, A. L. J.; Zavitsas, A. A. *Phys. Chem. Chem. Phys.* **2010**, *12*, 9597−9610. (b) Menon, A. S.; Wood, G. P. F; Moran, D.; Radom, L. *J. Phys. Chem. A* **2007**, *111*, 13638−13644. (c) Poutsma, M. L. *J. Org. Chem.* **2011**, *76*, 270−276. (d) Wood, G. P. F.; Moran, D.; Jacob, R.; Radom. *J. Phys. Chem. A* **2005**, *109*, 6318−6325.

(25) Hammond, G. S. *J. Am. Chem. Soc.* **1955**, *77*, 334−338.

(26) (a) Marcus, R. A. *Annu. Rev. Phys. Chem.* **1964**, *15*, 155−196. (b) Marcus, R. A. *J. Phys. Chem.* **1968**, *72*, 891−899. (c) For applications to reactions involving intermolecular hydrogen atom transfers, see ref 15b and Newcomb, M.; Manek, M. B.; Glenn, A. G. *J. Am. Chem. Soc.* **1991**, *113*, 949−958. For an application to radical cyclizations, see: (d) Alabugin, I. V.; Manoharan, M. *J. Am. Chem. Soc.* **2005**, *127*, 12583−12594. (e) Alabugin, I. V.; Timokhin, V. I.; Abrams, J. N.; Manoharan, M.; Abrams, R.; Ghiviriga, I. *J. Am. Chem. Soc.* **2008**, *130*, 10984−10995.

(27) For calculations referring to hydrogen abstraction by imide-*N*-oxyl radicals, see: Arnaud, R.; Milet, A.; Adamo, C.; Einhorn, C.; Einhorn, J. *J. Chem. Soc., Perkin Trans. 2* **2002**, 1967−1972 and references cited therein.

(28) The absolute configurations, resulting from retention of the configuration of the starting stereocenter, were assigned by analogy with our previous results; see ref 1.

(29) Stereochemistry was assigned from a NOESY experiment which showed cross-peaks between the proton α to the tosyl group at 5.95 ppm and the protons of the methyl group at 2.55 ppm.

(30) Effectively, the enantiomeric excess of naphthoazepine (2*R*,3*S*)-**33** formed in acetonitrile was only 65% instead of 84% in benzene.